Mechanistic studies on the decomposition of water soluble azo-radical-initiators

Roy U. Rojas Wahl,* Liansheng Zeng, Stephen A. Madison, Richard L. DePinto and Brian J. Shay

Unilever Research US, 45 River Road, Edgewater, NJ 07020, USA

Spin trapping with nitrones coupled with the use of electron paramagnetic resonance (EPR) is one of the most effective techniques to observe reactive radical oxygen species (RROS), even though the distinction between, for example, alkoxyl and alkylperoxyl radicals is not an easy task. In the light of this very problem, this work summarizes our results using three nitrones as spin traps and three water soluble amidino-azo-initiators as sources for alkylperoxyl and/or alkoxyl radicals. The principal conclusion of this study is that only the corresponding alkoxyl radicals were found to add to the nitrones, and no evidence was found for the alkylperoxyl radical-spin adducts. The spin traps 5-(diethoxyphosphoryl)-5-methyl-4,5-dihydro-3*H*-pyrrole *N*-oxide (DEPMPO) as well as methyl-*N*-durylnitrone (MDN) rendered a discriminative spin adduct assignment much simpler as compared to 5,5-dimethyl-4,5-dihydro-3*H*-pyrrole *N*-oxide (DMPO), where liquid chromatography–electrospray mass spectrometry (LC–ESMS) was employed to substantiate the EPR results. For the kinetic decomposition behavior of the azo initiators it was found that at pH 6.2 2,2′-azobis(2-methylpropionamidine) dihydrochloride (AAPH) undergoes hydrolysis to the corresponding amides while the cyclic initiators 2,2′-azobis[2-(2-imidazolin-2-yl)-propane] dihydrochloride (VA-44) and 2,2′-azobis{2-[2-(4-methyl)imidazolin-2-yl]propane} dihydrochloride (Me-VA-44) are resistant towards hydrolysis over the employed timescale of 30 h.

Introduction

Hydroxyl, hydroperoxyl/superoxyl and alkylperoxyl/alkoxyl radicals are very important reactive intermediates formed in the oxidation of many organic and biological materials.[1] For alkylperoxyl and/or alkoxyl radicals, however, little detail is known about the deleterious and/or beneficial events associated with either of these species. This is because the mechanistic distinction between those effects that are caused by an alkylperoxyl radical and those effects that are caused by an alkoxyl radical is not an easy task, for example because the former species can rapidly self-react to form the latter one. Consequently, many reports are based on conventional wisdom rather than mechanistic evidence. With electron paramagnetic resonance (EPR) and liquid chromatography–electrospray mass spectrometry (LC–ESMS) as the analytical tools, this contribution wishes to address this problem using three nitrone spin traps and three water soluble amidino-azo-initiators that are widely employed for radical polymerization as well as generators of oxidative stress in biological systems.

Azo-Radical Initiators:

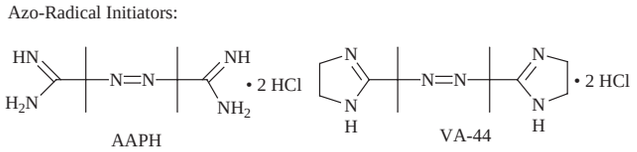

Spin Traps:

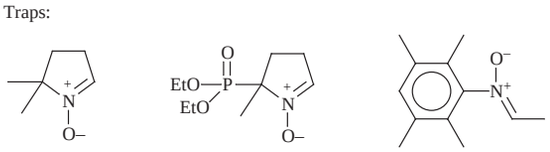

Azo-radical-initiators

The widely accepted mechanism for the thermal decomposition of azo-initiators is shown in Scheme 1. Due to usually low

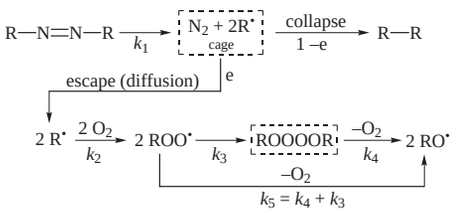

Scheme 1

values for k_1 ($\approx 10^{-7}$–10^{-6} s^{-1}) and near diffusion controlled values for k_2 ($\approx 10^9$ M^{-1} s^{-1}),[2] azo-initiators generate a constant flux of alkylperoxyl radicals ROO•, provided that sufficient initial amounts of azo-compound and an abundant oxygen supply are available throughout the entire timescale of the reaction. The head-to-head termination reaction of alkylperoxyl radicals is thought to give a tetroxide intermediate, which is in equilibrium with the peroxyl radicals at low temperature in organic solvents.[3] In aqueous solutions, tetroxides have not been observed, and these reactions exhibit second-order kinetics exclusively. The situation in mixed solvent systems (aqueous–organic) has yet to be clarified. The existence of tetroxides as intermediates would have made itself noticeable by the presence of a significant amount of a first-order component in the second-order kinetic scheme of product formation. We have chosen tertiary azo-initiators because the oxygen centered intermediates that are formed in the decomposition pathway do not bear an α-proton, which could give rise to side reactions such as the Russell reaction of the tetroxide[4] or proton shifts of the alkoxyl radical. The only side reaction of relevance for tertiary alkoxyl radicals is the well known β-scission leading to an alkyl radical and ketone. The polarity of the solvent has a profound impact on the rate of this reaction,[5] reaching a maximum in water ($k_\beta > 10^6$ s^{-1}).[6] Furthermore, structural differ-

ences of the radical species in question have to be considered, and the fastest rearrangement known is that of 2-methyl-1-phenyl-2-propyl hydroperoxide (MPPH) with $k_\beta = 2.2 \times 10^8$ s^{-1} (measured in CH_3CN).[7] The critical step in the reaction sequence in Scheme 1 is the recombination of the two alkylperoxyl radicals which gives two alkoxyl radicals. Typical values for tertiary alkylperoxyl radicals range from $k_5 \leqslant 2 \times 10^7$ dm^3 mol^{-1} s^{-1} for the radical derived from isopropyl ether[8] to $k_5 = 1.7$–2.0×10^4 dm^3 mol^{-1} s^{-1} for tertiary radicals derived from cumene or α-methylstyrene.[9,10]

Nitrone spin traps

5,5-Dimethyl-4,5-dihydro-3*H*-pyrrole *N*-oxide (DMPO) is one of the most frequently employed spin traps in organic and biological chemistry, mainly due to its solubility in both water and most organic solvents and also due to its superior ability to trap oxygen centered radicals when compared with nitroso compounds or other nitrones. It should be mentioned that DMPO spin trapping can in some instances be problematic due to the appearance of artificial signals derived from impurities[11] and/or when metals are involved.[12] Certain buffer solutions were found to overcome most of these obstacles.[13] Furthermore, DMPO–peroxyl spin adducts have been found to be of limited stability,[14] which prompted several authors to synthesize new and better DMPO derivatives.[15] For azo-initiators, double adduct formation derived from trapping of the alkyl radical by the preformed aminoxyl radical has been reported.[16] Although the vast majority of the studies have been carried out with hydroxyl and hydroperoxyl/superoxyl radicals,[17,18] a recent report by Krainev and Bigelow advertized the usefulness of the DMPO spin trap when reacted with 2,2′-azobis(2-methylpropionamidine) dihydrochloride (AAPH). The observed spin adduct was assigned as the DMPO–OR, and no evidence for the DMPO–OOR adduct was found.[2] As can be seen from Schemes 1 and 2, the rate constant k_5 is in direct competition with k_{trap},

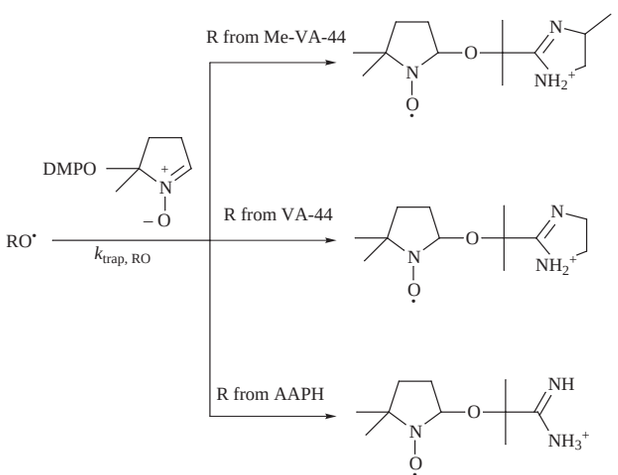

Scheme 2

the rate constant that represents the trapping reaction of alkylperoxyl radicals with the spin trap. Published literature values for the latter reaction are in the range of $k_{trap,ROO} = 7.72 \times 10^2$ dm^3 mol^{-1} s^{-1} to $k_{trap,ROO} = 6.56 \times 10^3$ dm^3 mol^{-1} s^{-1} for lauroyl peroxide in the case of substituted aromatic nitrones (electron acceptor substituents lead to higher rate constants),[19] but for DMPO nothing has been published to the best of our knowledge. The assignment of the nature of the oxygen centered spin adduct is not easy when using DMPO. The EPR spectral differences are small and usually based on computer simulated line shape fittings[2] and the frequent observation that DMPO–OR adducts exhibit a slightly larger $a_{\beta\text{-H}}$ splitting than the a_N splitting (for DMPO–Bu′O: $a_N = 14.85$ G and $a_{\beta\text{-H}} = 16.40$), in contrast to the DMPO–OOR adduct (for DMPO–Bu′OO: $a_N = 14.25$ G and $a_{\beta\text{-H}} = 10.55$).[20,21] Furthermore, it was found that in aqueous phosphate buffer solution the DMPO–Bu′OO spin adduct decays within 24 minutes and gives rise to the DMPO–Bu′O spin adduct.[20,22] These limitations lead investigators to develop spin traps other than DMPO. 5-(Diethoxyphosphoryl)-5-methyl-4,5-dihydro-3*H*-pyrrole *N*-oxide (DEPMPO) was reported to give OOH adducts that are up to 15 times more stable than the corresponding DMPO adduct. The additional a_P hyperfine splitting was said to be characteristic for the nature of the radical added, and the appearance of the entire spectrum exhibited a characteristic 'fingerprint' for the DEPMPO–OOH adduct.[23] Hence, DEPMPO may be a helpful spin trap for RO•/ROO• differentiation, assuming that HO• (HOO•) gives rise to a similar a_P hyperfine splitting to RO• (ROO•). Moreover, the use of methyl-*N*-durylnitrone† (MDN) also appears to be promising because this spin trap has already been employed to differentiate between RO• and ROO• in the open literature.[24–26] The only drawback is the sensitivity of the MDN–OOR spin adduct towards light[27] and the insolubility of the spin trap in aqueous media.

Results and discussion

Initially, the kinetic decomposition behavior of the azo-initiators was followed spectrophotometrically and the spin adduct formation was visualized by EPR using DMPO as a spin trap. For further confirmation of the spin adduct assignment (RO• *vs.* ROO•), DEPMPO and MDN were employed. Furthermore, in an interdisciplinary approach, liquid chromatography–mass spectrometry was utilized for the unequivocal identification of the spin adducts of DMPO.[28]

Decomposition behavior of azo-initiators: spectrophotometric studies

First, the decomposition behavior of the azo-initiators was studied by UV spectrophotometry. The decrease in the peak area at 365 nm (−N=N− chromophore) was used to determine the rate constants.

AAPH. At pH 7.2 in phosphate buffer, about 20% of AAPH decomposes within the first 6 h, with no apparent change in the peak area at $t \geqslant 6$ h at either room temperature or at 40 °C. Closer inspection of the decomposition of AAPH revealed that in addition to homolytic processes, AAPH undergoes hydrolysis to amide products (separated by LC and identified by ESMS). The amide products essentially do not undergo homolysis under the conditions that AAPH does and since the amido materials still contain the azo chromophore, their presence obfuscated following the disappearance of AAPH. Therefore, the decomposition of AAPH was monitored by LC–UV. This way, the AAPH decomposition could be decoupled from build up of the hydrolysis products. With this approach the first order rate constants for AAPH decomposition and appearance of hydrolysis products were determined to be $k_{1,AAPH} = 4.82 \times 10^{-5}$ s^{-1} (see Fig. 1) and $k_{hydr} = 4.60 \times 10^{-5}$ s^{-1} (see Fig. 2), respectively. From these studies it is evident that the steady state concentration of radicals formed by this initiator must be relatively low, because the hydrolysis products are stable towards decomposition under our conditions and do not contribute pivotally to radical formation. The undesirable hydrolysis of AAPH led to the investigation of two cyclic homologues as alternative radical initiators with the expectation that cyclic materials would be less prone to hydrolysis. In many cases it can be shown that ring closure is competitive with hydrolysis ($k_r \geqslant k_{hyd}$, see Scheme 3). Moreover, such cyclic compounds have been

† IUPAC name for methyl-*N*-durylnitrone is *N*-ethylidene(2,3,5,6-tetramethylphenyl)amine *N*-oxide.

Table 1 Average decomposition results of AAPH[a]

	Average decomposition rate for 5 h reaction/s^{-1}	AAPH decomposed after 5 h (%)
pH 7.2	6.24×10^{-6}	≈15
pH 7.2 + DMPO	2.20×10^{-7}	≈0.33
pH 11	1.16×10^{-5}	≈22
pH 11 + DMPO	1.29×10^{-6}	≈2.5

[a] Conditions: 10 mL of K_2HPO_4–KH_2PO_4–KCl buffer, 2.5 mmol AAPH, 40 °C, air. UV-spectra were taken at 365 nm every 2 h.

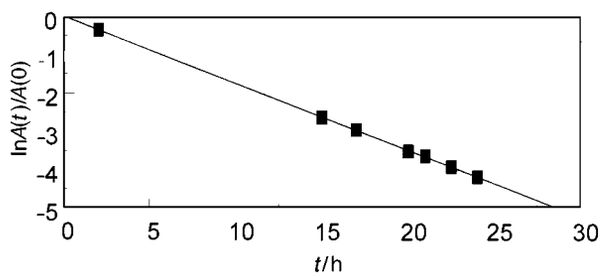

Fig. 1 Decomposition of AAPH. Conditions: [AAPH] 20 mM in water, pH 6.20, room temperature; rate constant $k_1 = 4.82 \times 10^{-5}$ s^{-1}; monitored by LC (H_2O–MeCN 75 : 25) and change in peak areas at 365 nm.

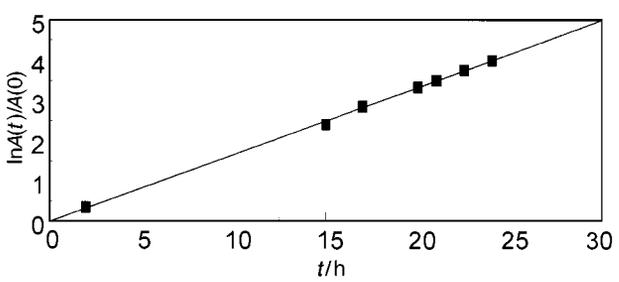

Fig. 2 Build up of AAPH-hydrolysis products. Conditions: [AAPH] 20 mM in water, pH 6.20, room temperature; rate constant $k_1 = 4.60 \times 10^{-5}$ s^{-1}; monitored by LC (H_2O–MeCN 75 : 25) and change in peak areas at 365 nm.

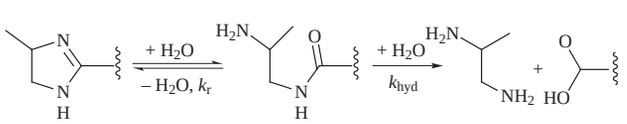

Scheme 3 Competition amide hydrolysis *vs*. ring closure

described in the literature to decompose faster than AAPH,[29] which, as we believed, would give us higher yields of spin adduct with DMPO. It was anticipated that this would render the detection of the spin adducts by means of mass spectrometry much easier. The presence of the spin trap DMPO leads to a significant decrease in the rate of decomposition of AAPH, and Table 1 shows some average decomposition rates for the first 5 h of decay determined by simple UV experiments without LC separation. At this time there is no convincing conclusion why DMPO slows down the rate of decomposition of AAPH, but it can be speculated that DMPO and AAPH form stabilized adducts in solution. More studies with AAPH, but also with other initiators, will be necessary to address this interesting observation.

VA-44. 2,2′-Azobis[2-(imidazolin-2-yl)propane] dihydrochloride (VA-44) was chosen because it is a known polymerization initiator and hence relatively inexpensive and readily available. As outlined above, this cyclic analog of AAPH was expected to be more hydrolytically stable. In water at pH 6.25, the first order rate constant for decomposition was found to be

Table 2 Typical hyperfine splitting constants for DMPO derived spin adducts of azo initiators[a]

Initiator	a_N/G	$a_{\beta\text{-H}}$/G	$a_{\gamma\text{-H}}$/G
AAPH	14.47	14.84	n.r.[b]
VA-44	14.14	14.52	n.r.[b]
Me-VA-44	14.08	14.51	n.r.[b]

[a] Conditions: room temperature (≈22 °C), flask open to air. DMPO (0.25 mmol) is dissolved in 5 mL potassium chloride–potassium phosphate buffer (pH 7.2), which has been flushed with O_2 for 10 minutes prior to its use. In each case, the initiator (0.375 mmol) is dissolved readily and an aliquot is taken out and placed in the EPR cavity. Instrumental: Bruker 300, ST_320 Resonator. Settings: receiver gain 5×10^5; modulation frequency 100 kHz; modulation amplitude 1 G or 0.635 G (see footnote *c*); conversion time 81.92 ms; time constant 10.24 ms; microwave power 24 mW; frequency 9.81 GHz; center field 3480 G; sweep width 200 G; number of scans 5. [b] Not resolved, even after the modulation amplitude was decreased down to 0.101 G. [c] Except for the sensitivity, in no case did a change in modulation amplitude have any observable impact on the appearance of the spectra or the hyperfine splitting(s). It should be noticed here, that in water, DMPO spin adducts typically exhibit broader lines unsuitable for obtaining typical fingerprint spectra for a given adding radical (see ref. 40). Also MDN and DEPMPO were found to exhibit a similar behavior.

Fig. 3 EPR of DMPO–OR spin adduct (R from AAPH)

$k_{1,VA44} = 7.5 \times 10^{-6}$ s^{-1}. No hydrolysis products were observed by LC and ESMS.‡

Me-VA-44. 2,2′-Azobis{2-[(4-methyl)imidazolin-2-yl]propane} dihydrochloride (Me-VA-44) decomposes in water at pH 6.25 following a first order process with $k_{1,MeVA44} = 1.6 \times 10^{-5}$ s^{-1}. The synthesis of this compound followed standard synthetic methods.[30]

ROO• *vs* RO•: nitrone-spin adduct assignment using EPR

The formation of the spin adducts was investigated by EPR. The spin trapping reaction is outlined in Scheme 2 for the example of RO• and DMPO. All spin adducts exhibited shifts of $g = 2.0084$.

DMPO. A typical EPR spectrum using DMPO is shown in Fig. 3 for the spin adduct with the AAPH derived radical. Typical hyperfine splittings observed for all three initiators are summarized in Table 2. The $a_{\beta\text{-H}}$ hyperfine splittings of all three initiators are slightly larger than the corresponding a_N splitting. This is a first evidence that the nitrone is trapping the alkoxyl radical (RO•) derived from recombination of two alkylperoxyl radicals (ROO•, see Scheme 1). These hyperfine splittings do not change with time, hence there is no visible EPR evidence that the alkylperoxyl radicals themselves are trapped to a significant extent. The build-up of the DMPO–spin adducts of all three initiators was followed quantitatively with time, and the results are depicted in Fig. 4. Interestingly, from $t = 1$ h on, the concentration of the DMPO–OR adduct (R derived from AAPH) is constantly higher than the one from the other two initiators. It has to be mentioned that in the cases of VA-44 and

‡ Instead, MS-evidence for β-scission to form the ketone was found.

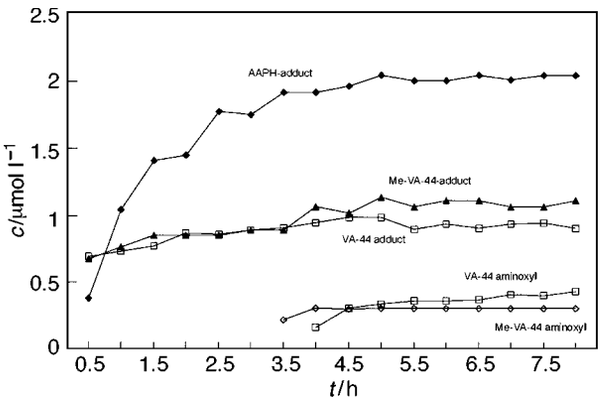

Fig. 4 DMPO–OR spin adduct profile by EPR. Conditions: 4-HO-TEMPO as external standard; [DMPO] 50 mM, [Initiator] 75 mM, 5 ml KCl–K-phosphate buffer pH 7.2, room temperature, 22 °C, air. Buffer was flushed with oxygen for 10 min prior to use. AAPH: Reaction followed in capillary within cavity. Others: Reaction followed by taking aliquots from stirring flask into capillary.

Me-VA-44, the usual DMPO–OR signal starts to be accompanied by a triplet signal from $t = 3.5$ and $t = 4$ h on, respectively. This signal has the following hyperfine couplings: a_N = 13.5 G and $a_{\gamma\text{-H}}$ = 1.4 G. There is no $a_{\beta\text{-H}}$ splitting. This is indicative of an aminoxyl radical without β-hydrogen. These data are significantly distinct from those observed for a hypothetical DMPO–OX species,[17] and therefore at this time it can only be speculated about the origin of this signal. Limited O_2 supply may play a role here, because this signal appeared sooner when the reaction was followed in the EPR capillary as compared to when the reaction was followed in the flask (with stirring) outside of the cavity. However, performing an experiment under argon only gave the formation of the corresponding DMPO–R spin adduct ($a_{\beta\text{-H}}$ = 22 G, typical for a carbon centered radical adding to the nitrone), and no evidence for the removal of the β-hydrogen could be found as no triplet was observed. A possible explanation for the appearance of the aminoxyl triplet may be the disproportionation of the DMPO–spin adduct forming the hydroxylamine and the C-2 substituted 3*H*-pyrrole *N*-oxide [2 −CHR−N(R′)O$^\bullet$ ⟶ −CHR−N(R′)OH and −CR=N(R′)O]. The latter can be attacked by a second radical yielding an aminoxyl radical without β-hydrogen. Whether or not this second radical is oxygen (with subsequent superoxide formation) or derived from the radical initiator remains speculation at this time. An experiment using AAPH and DMPO in chelex treated buffer solution (removal of traces of metal ions) did result in the usual spin adduct formation ($a_{\beta\text{-H}}$ = 14.92 G, a_N = 14.57 G). Hence, traces of metals do not interfere with the results of this study. Another possible explanation for the triplet may be that the formation of alkoxyl alkyl aminoxyls, which has been reported previously for open chain nitrones,[14b] accompanied the formation of the corresponding carbonyl compounds.[14c]

DEPMPO. This spin trap gives a 'double DMPO-type spectrum', as can be seen for example of the corresponding Me-VA-44 adduct in Fig. 5(a). Table 3 gives typical hyperfine splitting constants for all three initiators. In contrast to DMPO, the $a_{\beta\text{-H}}$ splittings are smaller than the a_N splittings, and similar findings were reported for the DEPMPO–OH adduct. In addition, the a_P values are much closer to the corresponding value for DEPMPO–OH adduct than the DEPMPO–OOH adduct. Most importantly nothing of the characteristic fingerprint of the ROO$^\bullet$ adduct could be observed, even though this spin trap is known for exhibiting such fingerprints with HOO$^\bullet$ in aqueous solutions. One report shows exactly such a fingerprint for MeOO$^\bullet$ in the form of a computer simulation that assumes the existence of two diastereomers with two distinct a_P splittings for the DEPMPO–OOMe adduct.[23a,31] When DEPMPO was reacted with Co^{II}-acetylacetonate and Bu^{t}OOH (TBHP),§[27] the spectrum shown in Fig. 5(b) was obtained. In agreement with the literature,[23a] it exhibits the fingerprint characteristic for the DEPMPO–OOR (R = *tert*-butyl) adduct. The hyperfine splittings are shown in Table 3. The lack of fingerprints in the observed DEPMPO spectra with all three azo-initiators is therefore the strongest indication for RO$^\bullet$ as the trapped species.

MDN. This spin trap was synthesized according to available literature procedures,[32] and only the last step to yield MDN from nitrosodurene required modification of the published procedure[33] and is described in more detail in the Experimental section. The EPR experiments were, not unexpectedly, complicated by the very poor solubility of MDN in aqueous solutions.

Table 3 Typical hyperfine splitting constants for DEPMPO derived spin adducts of azo initiators[a]

	a_P/G	a_N/G	$a_{\beta\text{-H}}$/G	$a_{\gamma\text{-H}}$/G	Ref.
AAPH	46.30	13.35	12.73	n.r.[b]	this work
VA-44	46.31	13.40	12.74	n.r.[b]	this work
Me-VA-44	46.47	13.37	12.78	0.61	this work
DEPMPO–OH	47.4	14.0	13.0	0.27	23(*a*)
DEPMPO–OOH	52.5	13.4	11.9	0.8, 0.43	23(*a*)
DEPMPO–OOR[d]	49.19	12.51	10.12	n.r.	this work

[a] Conditions: Room temperature (≈22 °C), flask open to air. DEPMPO (0.25 mmol) is dissolved in 5 mL potassium chloride–potassium phosphate buffer (pH 7.2), which has been flushed with O_2 for 10 minutes prior to its use. In each case, the initiator (0.375 mmol) is dissolved readily and an aliquot is taken out and placed in the EPR cavity. Instrumental: Bruker 300, ST_320 Resonator. Settings: receiver gain 5×10^5; modulation frequency 100 kHz; modulation amplitude 1 G or 0.635 G (see footnote *c*); conversion time 81.92 ms; time constant 10.24 ms; microwave power 24 mW; frequency 9.81 GHz; center field 3480 G; sweep width 200 G; number of scans 5. [b] See Table 2. [c] See Table 2. [d] Experiment carried out in benzene–*tert*-butyl alcohol–phosphate-buffer–ethanol 1:1:1:2. The hyperfine splittings refer to the major conformer (see ref. 23*a*).

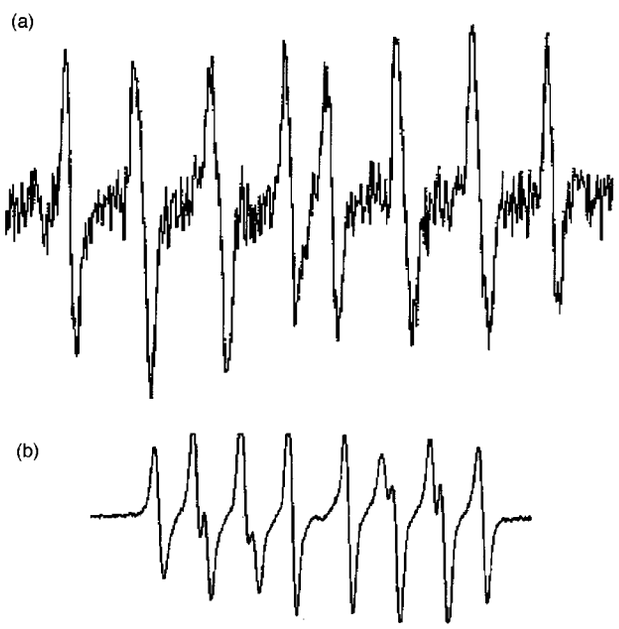

Fig. 5 (a) EPR of DEPMPO–OR spin adduct (R from Me-VA-44). (b) EPR of DEPMPO–OOR (R = Bu^t).

§ $$Bu^tOOH + Co^{2+} \rightarrow Bu^tO^\bullet + OH^- + Co^{3+} \quad (1)$$

$$Bu^tOOH + Co^{3+} \rightarrow Bu^tOO^\bullet + H^+ + Co^{2+} \quad (2)$$

The ratio TBHP/MDN is 25:1. Under these conditions, the intermediate Bu^{t}O$^\bullet$ abstracts a hydrogen from the excess TBHP and does not react significantly with the spin trap.

Table 4 Typical hyperfine splitting constants for MDN derived spin adducts of azo initiators[a]

	a_N/G	$a_{\beta\text{-H}}$/G	$a_{\gamma\text{-H}}$/G
VA-44	14.56	9.13	n.r.[b]
Me-VA-44	14.52	9.22	n.r.[b]

[a] Conditions: Room temperature (≈22 °C), flask open to air, but protected from light. MDN (0.25 mmol) and 0.375 mmol initiator are dissolved in mixture of 2 mL benzene, 2 mL Bu^{t}OH, 4 mL EtOH and 2 mL potassium chloride–potassium phosphate buffer (pH 7.2). This system was flushed with O_2 for 10 minutes prior to its use. For the measurement, an aliquot is taken out rapidly and placed in the EPR cavity, which is protected from light. Instrumental: Bruker 300, ST_320 Resonator. Settings: receiver gain 5×10^5; modulation frequency 100 kHz; modulation amplitude 1 G or 0.202 G (see footnote *c*); conversion time 81.92 ms; time constant 10.24 ms; microwave power 24 mW; frequency 9.81 GHz; center field 3480 G; sweep width 200 G; number of scans 5. [b] See Table 2. [c] See Table 2.

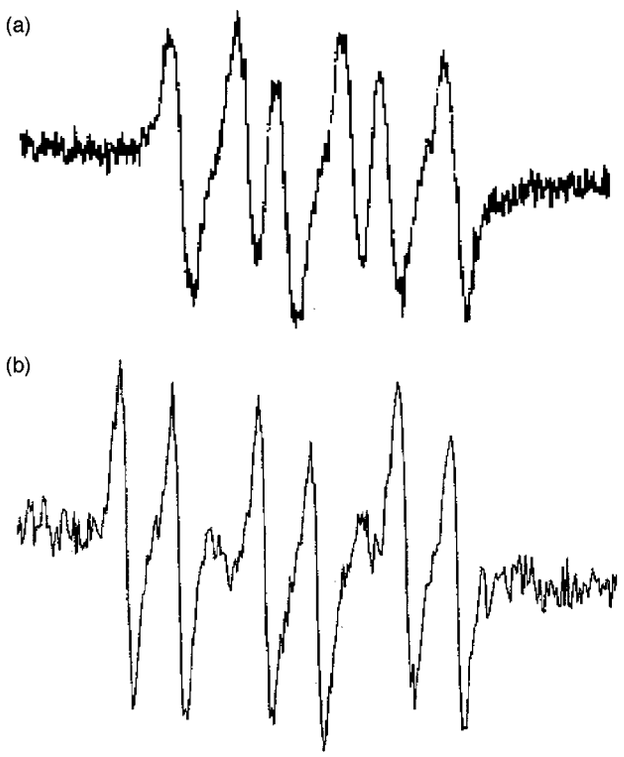

Fig. 6 (a) EPR of MDN–OR (R from VA-44). (b) EPR of MDN–OOR (R = Bu^t) spin adduct.

AAPH and MDN did not react at all, and no radicals could be detected, even though a variety of solvent mixtures were tried. Fortunately, the situation changed for VA-44 and Me-VA-44. Both initiators gave almost identical spectra in a mixture of benzene, Bu^{t}OH, EtOH and buffer solution. The spectrum of the MDN–OR (R derived from VA-44) is shown in Fig. 6(a), and Table 4 lists the observed hyperfine splittings. Even though the obtained spectra are broad and of low intensity, the hyperfine splittings are clearly indicative of an alkoxyl radical as the attacking species. The a_N splittings of 14.56 G (VA-44) and 14.52 G (Me-VA-44) indicate aminoxyl radicals. Most importantly, the obtained $a_{\beta\text{-H}}$ splittings of 9.13 G (VA-44) and 9.22 G (Me-VA-44) are in good agreement with corresponding literature data obtained for Bu^{t}O radicals.¶[24] A blank experiment was carried out in the same solvent system as described in Table 4. Co^{II}-acetylacetonate and Bu^{t}OOH (TBHP) were used as a reliable source of Bu^{t}OO radicals,§[28] and the obtained spectrum [Fig. 6(b)] showed an a_N of 13.44 G and an $a_{\beta\text{-H}}$ of 4.86 G, even though it was soon overlapped with the characteristic signal (triplet, $a_N = 7.14$ G, spectrum not shown) of MDN–OX (*N*-aceto-*N*-duryl aminoxyl). This phenomenon is known for PBN when metals are used to generate ROO$^{\bullet}$.[34] The $a_{\beta\text{-H}}$ of 4.86 G value is still significantly below the values of around 9.2 (see Table 4) and close to what is reported in the literature for the MDN–OOR spin adduct (*e.g.* 4.76).[24] Hence, when reacted with VA-44 and Me-VA-44 in the presence of oxygen, this spin trap provides clear evidence for the corresponding alkoxyl radicals as the major components attacking the nitrone moiety.

¶ In order to get both the initiator and the spin trap into solution, it was necessary to use the solvent system as described in Table 4. However, it was found, that increasing amounts of the aqueous buffer solution lead to an increase of the $a_{\beta\text{-H}}$ splitting. The ranges were 8.15 to 11.2 G. This may be due to conformational changes induced by hydrogen bonding.

Confirmation of DMPO–spin adduct assignments with LC–ESMS[35]

AAPH. A 10 μL aliquot of the AAPH–DMPO reaction (75 mmol AAPH, 50 mmol DMPO, KCl, KH_2PO_4 buffer, pH 7.2, room temp. 22 °C, pre-purged with O_2) was separated on an Inertsil ODS2 column (150 × 2 mm) with a mobile phase of 10 mM ammonium acetate and acetonitrile using gradient elution at 200 μL min^{-1}. The gradient program was 2% acetonitrile for 5 minutes to 70% acetonitrile in 10 minutes, then hold for 5 minutes. The LC effluent was directed into the mass spectrometer (Finnigan-MAT LCQ). All the analytes formed M + H$^+$ ions under the system conditions. AAPH and DMPO eluted early while a spin adduct corresponding to the DMPO–OR (R = AAPH alkyl radical) addition product eluted after 16 minutes. Fig. 7(a) shows the chromatogram of the reaction mixture after 2 hours with the corresponding mass spectrum for the spin adduct (*m*/*z* 215, MH$^+$) at $t_R = 16.27$ min. MS–MS experiments used LC, direct injection, and direct infusion (10 μL min^{-1}) of the isolated chromatographic peak. MS–MS fragmentation of *m*/*z* 215 by flow injection shows predominantly *m*/*z* 86 corresponding to the AAPH tertiary radical (protonated). This and other characteristic fragment ions are depicted in Fig. 7(b).

VA-44. The VA-44–DMPO reaction mixture (10 μL) was separated with gradient chromatography on a Spherisorb ODS2 column 250 × 4.6 mm using 1 mL min^{-1} (unsplit to MS) of 3 mM ammonium acetate–acetonitrile as the mobile phase. The gradient conditions were 0% acetonitrile to 95% in 5 minutes. An ion at *m*/*z* 241 was detected, which corresponds to the spin adduct DMPO–OR (R = VA-44 alkyl radical) M + H$^+$ of the DMPO–OR spin adduct. Fig. 8(a) shows the chromatogram of the reaction mixture identifying the reactants, spin adduct and the mass spectrum of the spin adduct. The spin adduct was further characterized by MS–MS experiments. Fig. 8(b) displays the LC-MS–MS spectrum of the 241 ion and a depiction of the fragmentation pathways. Of note is the adduct fragment ion observed at *m*/*z* 113, the DMPO$^{\bullet+}$ radical cation by loss of ROH.

Me-VA-44. The Me-VA-44–DMPO reaction mixture (10 μL) was separated on an Isco Allspher ODS column 250 × 4.6 mm. An isocratic mobile phase was employed consisting of 75/25 water–acetonitrile at 1 ml min^{-1} unsplit to MS. A peak with a *m*/*z* = 255 was observed corresponding to the DMPO–OR (R = Me-VA-44 alkyl radical) addition product (protonated). Fig. 9(a) shows a chromatogram and mass spectrum of the reaction mixture. The spin adduct was further characterized by MS–MS experiments. Fig. 9(b) shows the flow injection MS–MS spectrum of the 255 ion. Characteristic ions at *m*/*z* 126 (loss of DMPO–O) and 142 (loss of DMPO) were the salient features. In the mass spectrum [Fig. 9(a)] the ion at 256 may correspond to the reduced form of the spin adduct (proton uptake) and the ion at 254 may correspond to the oxidized form of the spin-adduct (loss of β-hydrogen). This has been reported previously in the literature.[36] Further characterization was not pursued. These ions were present in the MS–MS spectrum [Fig. 9(b)] due to the wide mass isolation window of the parent ion.

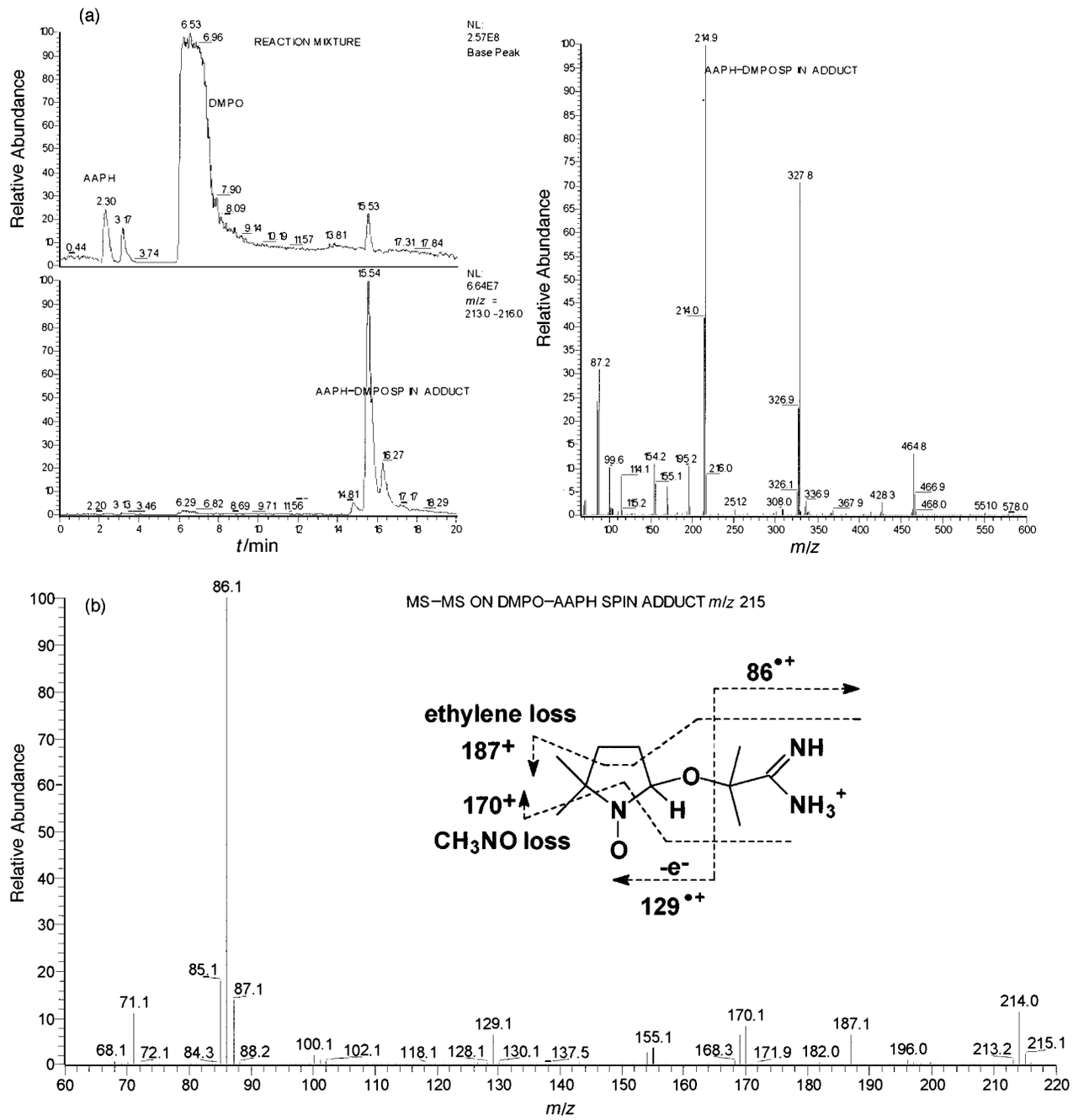

Fig. 7 (a) AAPH + DMPO: Base peak and selected ion (*m*/*z* 215) chromatograms of reaction mixture and MS of spin adduct. (b) DMPO–OR (R from AAPH): MS–MS.

Conclusions

We have employed three amidino-azo-initiators and three nitrone spin traps in order to distinguish between alkoxyl and alkylperoxyl radicals adding to these nitrones.

Except for the case of AAPH with MDN where no reaction was observed at all, the three nitrone spin traps react with the alkoxyl radicals derived from these three initiators. In the presence of these spin traps, no evidence for β-scission of the alkoxyl radicals is found. Furthermore, no evidence is found for trapping the corresponding alkylperoxyl radicals. In principle however, the presence of the corresponding peroxyl spin adducts can only be ruled out by lack of evidence. LC–ESMS and two nitrone spin traps (MDN and DEPMPO) have been identified as particularly useful tools for discriminating alkoxyl spin adducts from alkylperoxyl spin adducts. In contrast to the cyclic azo-initiators VA-44 and Me-VA-44, the acyclic azo-initiator AAPH hydrolyzes under the reaction conditions employed.

These results should prove to be of significance for future mechanistic studies in autooxidation processes, lipid peroxidation, protein peroxidation and in studies that employ AAPH as a source of free radicals in polymerization chemistry as well as in biological systems.

Experimental

General

All chemicals were used as purchased from Aldrich, except DMPO, which was filtered from milli-Q-water (Millipore) over charcoal prior to use. DEPMPO was obtained from Oxis International Inc. and VA-44 was provided by Wako Chemicals.

EPR

All EPR experiments were performed in a Bruker 300 using a ST_320 cavity. *g*-Values were determined against 2,2-di(4-*tert*-

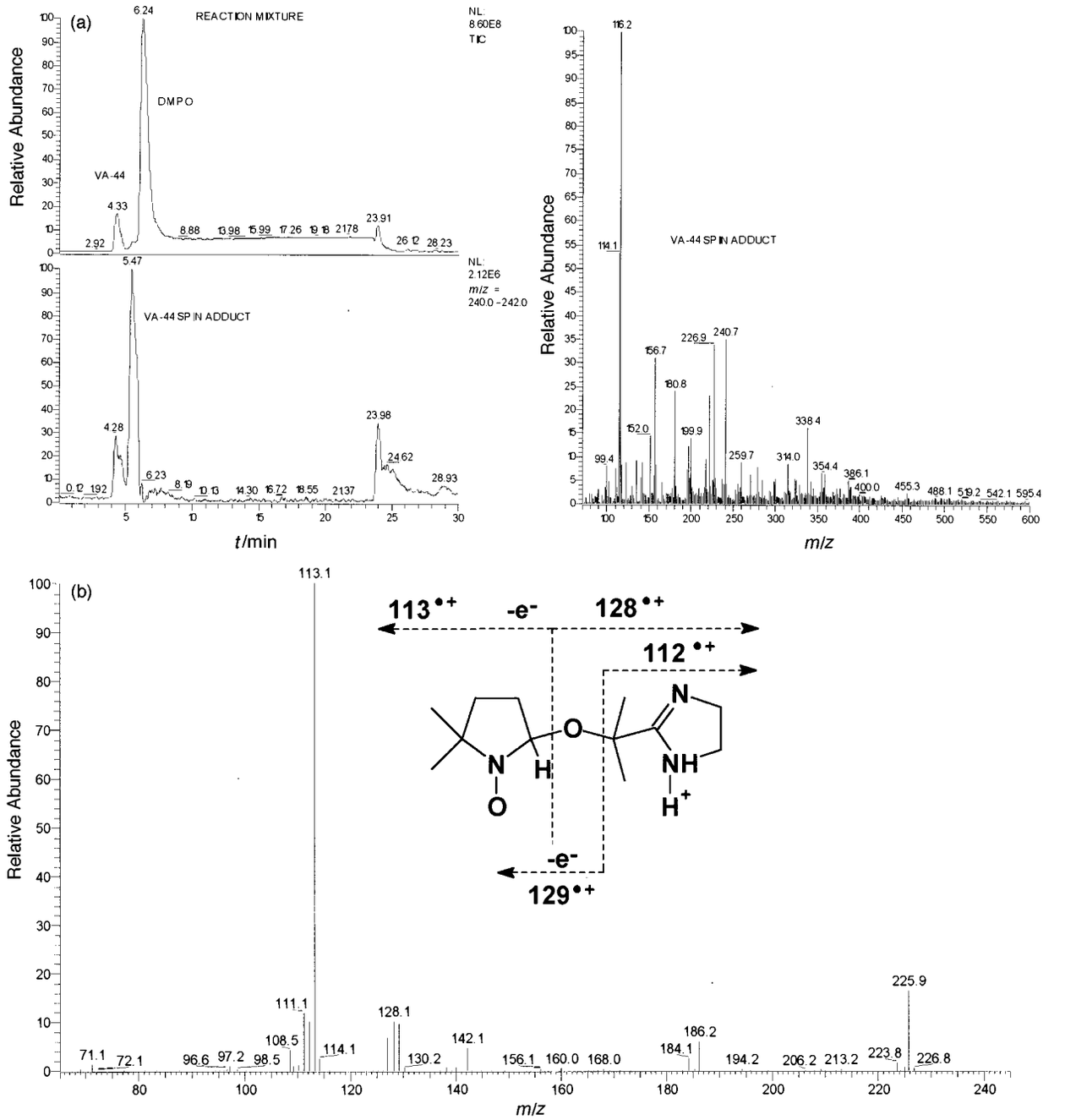

Fig. 8 (a) VA-44 + DMPO: Total ion current and selected ion (*m*/*z* 241) chromatograms of reaction mixture and MS of spin adduct. (b) DMPO–OR (R from VA-44): MS–MS.

octylphenyl)-1-picrylhydrazyl free radical (DPPH) in benzene ($g = 2.0035$)[37] as an external standard.

UV-initiator decomposition studies

All experiments were carried out using a Hewlett Packard 8452A Diode Array Spectrophotometer.

LC-initiator decomposition studies

All LC separations were performed on a Waters, LC module 1 using a Waters 996 PDA detector. For AAPH, a Hamilton PRP Polymeric Column 150 × 4.1 mm was used. VA-44 and Me-VA-44 were studied using an ISCO ODS II (C18, 4.6 mm × 250 mm) reversed-phase column. The volume of injection was 10 μL.

LC–MS

The spin trap adducts for the various initiators with DMPO were characterized by liquid chromatography–ion trap mass spectrometry (LC–ITMS) using positive ion electrospray ionization (ESI). All work was performed on a Finnigan MAT Ion Trap Mass Spectrometer (LCQ) using a 5 kV spray voltage and 200 °C capillary inlet. The reaction mixtures were separated using reversed-phase liquid chromatography. Specific LC details are given in the text. MS–MS experiments were performed by direct infusion of the reaction mixture or LC-collected fractions into the mass spectrometer within 10 minutes of collection and without further dilution. MS–MS parent ions were isolated with a mass window of 2 Daltons to obtain sufficient signal for subsequent fragmentations.

Methyl-*N*-durylnitrone (MDN) synthesis

(*a*) *Nitrosodurene* was synthesized in two steps according to the methods described in the literature.[32] Overall yield: 0.8265 g (5.06 mmol, 39%), white needles, mp 154 °C. Due to lack of NMR data in the literature, they are given here: $\delta_H(CDCl_3)$ 7.11 (s, 1 H), 2.31 (s, 6 H), 2.28 (s, 6 H); $\delta_C(CDCl_3)$ 142.22, 134.42,

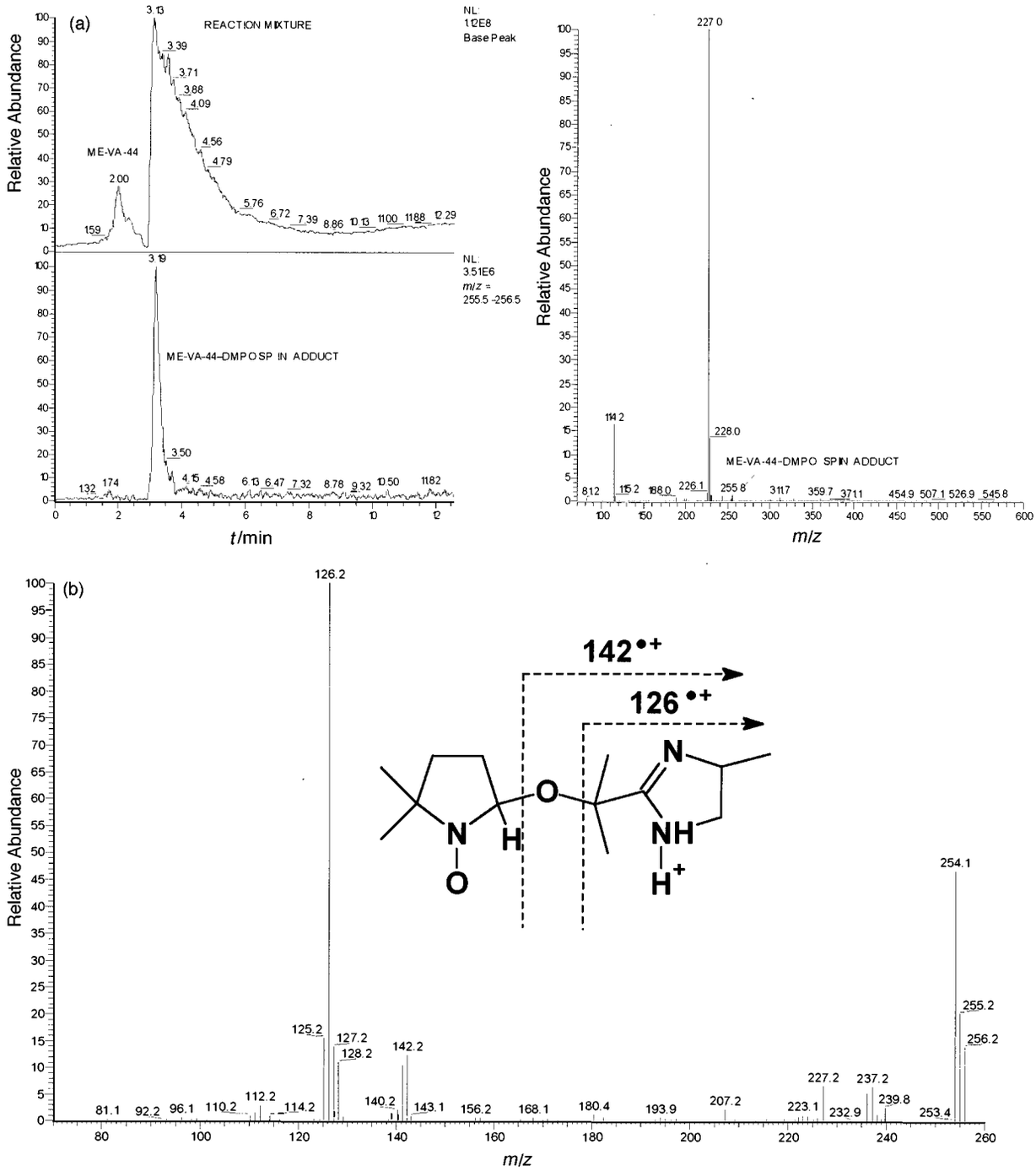

Fig. 9 (a) Me-VA-44 + DMPO: Base peak and selected ion (*m*/*z* 256) chromatograms of reaction mixture and MS of spin adduct. (b) DMPO–OR (R from Me-VA-44): MS–MS.

128.41, 126.77, 19.84, 15.26 (Found: C, 73.29; H, 8.05; N, 8.54. $C_{10}H_{13}NO$ requires: C, 73.59; H, 8.03; N, 8.58%).

(*b*) *MDN:* 0.8265 g (5.06 mmol) of nitrosodurene were dissolved under N_2 atmosphere in 40 mL of $CHCl_3$. 3.114 g (17.55 mmol) of *N*-nitroso-*N*-ethylurea (66%) was purified and dried according to a standard procedure,[38] where however 50 mL diethyl ether was used instead of light petroleum. The dry etheral solution was added slowly to the nitrosodurene solution at 0 °C. After initial reflux (*ca*. 30 min) the mixture was left for 2 h at room temperature and then the solvent was evaporated. The yellow–white solid residue was taken up in a minimum amount of ethyl acetate and flashed over silica gel ($R_{F_{(EtOH)}}$: 0.72). Four fractions were collected, the solvent evaporated and the solids high vacuum dried. Fraction three was analyzed. Yield after recrystallization (light petroleum): 0.4912 g (2.61 mmol, 51%), white leaflets (slightly yellowish), mp 89 °C (in agreement with ref. 25). $\delta_H([^2H_6]$acetone) 6.99 (s, 1 H), 6.93 (q, *J* 5.91 Hz, 1 H), 2.22 (2s, strongly overlapped, 6 H), 2.11 (d, *J* 5.91, 3 H), 2.08 (2s, strongly overlapped, 6H); $\delta_C([^2H_6]$-acetone) 148.2, 137.0, 135.9, 133.1, 127.7, 19.8, 14.1, 12.5; λ_{max}(EtOH)/nm 241 (consistent with absence of aromatic conjugation, which is sterically inhibited by *ortho*-methyl groups); ν(KBr)/cm^{-1} (ATR–FTIR) (w = weak, m = medium, s = strong, vs = very strong) 3075.9 (w), 3002.62 (m), 2967.91 (s), 2940.91 (s), 2921.63 (s), 2861.84 (m), 1585.20 (vs, indicates the presence of a polarized double bond in non-conjugation with aromatic ring), 1481.06 (s), 1446.35 (s), 1346.07 (vs), 1157.08 (s), 1103.08 (s), 1058.73 (vs), 1008.73 (s), 867.81 (m), 736.67 (m).

Me-VA-44 synthesis

(*a*) The free imino ether $MeOC(NH)C(CH_3)_2N{=}NC(CH_3)_2$-C(NH)OMe was prepared in quantitative yields in two steps

from AIBN following the conditions of a standard literature procedure.[39]

(*b*) The cyclization of the imine ether was carried out as follows: 0.18 mL (2.1 mmol) 1,2-diaminopropane were dissolved in 5 mL MeOH. After 5 minutes stirring, 0.2502 g (1.0 mmol) of free imino ether, dissolved in 0.5 mL toluene, were added and the mixture left for one day. Concentrating and storage at −20 °C yielded a light yellow solid, which was filtered off and vacuum dried for 2 h. Yield: 0.2214 g (0.8 mmol, 80%), mp 84.5–86 °C, λ_{max}(toluene)/nm 372; *m*/*z* (ESMS) 279 (M + H^+); $\delta_H(CDCl_3)$ 3.96 (m, 2 H), 3.75 (dd, *J* 11.4, 9.72, 2 H), 3.22 (dd, *J* 11.4, 7.02, 2 H), 1.44 (s, 12 H), 1.19 (d, *J* 6.28, 6 H); $\delta_C(CDCl_3)$ 169.56, 70.74, 70.72, 24.15, 24.06, 21.71.

(*c*) Hydrochlorination to form Me-VA-44: 0.2100 g (0.75 mmol) of the above solid was dissolved in MeOH and HCl gas was bubbled through the solution (about 5 g HCl was added). After 15 minutes 15 mL of acetone were added, and the white precipitate was filtered off and vacuum dried for 3 h. Yield: 0.2435 g (0.69 mmol, 92.2%). mp 154–157 °C. λ_{max}(water)/nm 365 (ε = 26.6 M^{-1} cm^{-1}); *m*/*z* (ESMS) 279 (M + H^+, Cl^- clusters in negative ion mode).

Acknowledgements

We thank Professor N. J. Turro, Columbia University, for providing the EPR facilities and Professor P. Tordo, University of Aix Marseille, for the kind supply of manuscripts. Dr A. G. Krainev, University of Kansas, is thanked for helpful comments.

References

1 The almost universal importance of these types of radicals may be best illustrated by the vast number of books, reviews and research articles that have appeared over the past decades. See for example the following, arbitrarily chosen four contributions and the references cited therein: (*a*) Z. Alfassi, ed., *Peroxyl Radicals*, Wiley, Chichester, 1997; (*b*) P. Neta, R. E. Huie and A. B. Ross, *J. Phys. Chem. Ref. Data*, 1990, **19**, 413; (*c*) J. K. Kochi, ed., *Free Radicals*, Vol. I and II, Wiley, Chichester, 1973; (*d*) K. U. Ingold, *Acc. Chem. Res.*, 1969, **2**, 1.

2 A. G. Krainev and D. J. Bigelow, *J. Chem. Soc.*, *Perkin Trans. 2*, 1996, 747 and references therein.

3 C. Von Sonntag and H. P. Schuchmann, *Angew. Chem. Int. Ed. Engl.*, 1991, **30**, 1229 and references therein.

4 G. A. Russell, *J. Am. Chem. Soc.*, 1957, **79**, 3871.

5 C. Walling and P. J. Wagner, *J. Am. Chem. Soc.*, 1964, **86**, 3368.

6 B. C. Gilbert, P. D. R. Marshall, R. O. C. Norman, N. Pineda and P. S. Williams, *J. Chem. Soc.*, *Perkin Trans. 2*, 1981, 1392.

7 I. W. C. E. Arends, K. U. Ingold and D. D. M. Wayner, *J. Am. Chem. Soc.*, 1995, **117**, 4710.

8 M. N. Schuchmann and C. von Sonntag, *Z. Naturforsch. B 42*, 1987, 495.

9 A. R. Costello, J. R. Lindsay Smith, M. S. Stark and D. J. Waddington, *J. Chem. Soc.*, *Faraday Trans.*, 1996, **92**, 3497 and references therein.

10 (*a*) J. A. Howard and K. U. Ingold, *Can. J. Chem.*, 1968, **46**, 2655; (*b*) J. A. Howard, K. Adamic and K. U. Ingold, *Can. J. Chem.*, 1969, **47**, 3793.

11 G. R. Buettner and L. W. Oberley, *Biochem. Biophys. Res. Commun.*, 1978, **83**, 69.

12 K. Makino, T. Hagiwara, A. Hagi, M. Nishi and A. Murakami, *Biochem. Biophys. Res. Commun.*, 1990, **172**, 1073.

13 P. M. Hanna, W. Chamulitrat and R. P. Mason, *Arch. Biochem. Biophys.*, 1992, **2**, 640.

14 (*a*) The DMPO–OOH adduct has chiefly been investigated due to its biological relevance. It was found to decompose and yield the DMPO–OH spin adduct. Most studies are qualitative, but for a quantitative investigation see: I. Yamazaki, L. Piette and T. A. Grover, *J. Biol. Chem.*, 1990, **265**, 652 and references therein. In general, alkylperoxy aminoxyls can decompose to yield alkoxy alkyl aminoxyls. See: (*b*) M. J. Perkins and B. P. Roberts, *J. Chem. Soc.*, *Perkin Trans. 2*, 1974, 297; (*c*) K. Hensley, M. Aksenova, J. M. Carney, M. Harris and D. A. Butterfield, *Neuro Report*, 1995, **6**, 493.

15 (*a*) For C-2 methyl substitution and ^{13}C-2 labelling see: D. Barasch, M. C. Krishna, A. Russo, J. Katzhendler and A. Samuni, *J. Am. Chem. Soc.*, 1994, **116**, 7319; (*b*) For C-2 phenyl substitution and ^{13}C-2 labelling see: E. G. Janzen, Y. K. Zhang and D. Lawrence Haire, *J. Am. Chem. Soc.*, 1994, **116**, 3738; (*c*) For C-2 ^{31}P-substitution see: E. G. Janzen and Y. K. Zhang, *J. Org. Chem.*, 1995, **60**, 5441; (*d*) For C-2 CF_3 substitution see: E. G. Janzen, Y. K. Zhang and M. Arimura, *J. Org. Chem.*, 1995, **60**, 5434. Note that C-2 substitution removes the β-H, and therefore abstraction of that hydrogen and subsequent disproportionation of the spin adduct is prevented, which should lead to higher stability.

16 E. G. Janzen, P. H. Krygsman, D. A. Lindsay and D. H. Haire, *J. Am. Chem. Soc.*, 1990, **112**, 8279. Notably, also LC–MS has been used to identify the spin adducts.

17 K. Makino, T. Hagikawa and A. Murakami, *Radiat. Phys. Chem.*, 1991, **37**, 657.

18 E. G. Janzen and D. L. Haire, *Adv. Free Radical Chem.*, 1990, **1**, 253.

19 A. Y. Gerchikov, I. S. Nasyrov, N. A. Akmanova, V. S. Martemiyanov and E. T. Denisov, *React. Kinet. Catal. Lett.*, 1987, **33**, 317.

20 W. Chamulitrat, N. Takahashi and R. P. Mason, *J. Biol. Chem.*, 1989, **264**, 7889 and references therein.

21 J. I. Ueda, N. Saito and T. Ozawa, *J. Inorg. Biochem.*, 1996, **64**, 197 and references cited therein.

22 M. J. Davies, *Biochim. Biophys. Acta*, 1988, **964**, 28.

23 (*a*) C. Frejaville, H. Karoui, B. Tuccio, F. LeMoigne, M. Culcasi, S. Pietri, R. Lauricella and P. Tordo, *J. Med. Chem.*, 1995, **38**, 258; (*b*) B. Tuccio, R. Lauricella, C. Frejaville, J. C. Bouteiller and P. Tordo, *J. Chem. Soc.*, *Perkin Trans. 2*, 1995, 295.

24 R. Konaka, S. Terabe, T. Mizuta and S. Sakata, *Can. J. Chem.*, 1982, **60**, 1532.

25 T. Yamada, E. Niki, S. Yokoi, J. Tsuchiya, Y. Yamamoto and Y. Kamiya, *Chem. Phys. Lipids*, 1984, **36**, 189.

26 B. Plesnicar, F. Kovac and M. Schara, *J. Am. Chem. Soc.*, 1988, **110**, 214.

27 E. Niki, S. Yokoi, J. Tsuchiya and Y. Kamaiya, *J. Am. Chem. Soc.*, 1983, **105**, 1498.

28 In a recent contribution, liquid chromatography–mass spectrometry is used for the characterization of the DMPO–OR spin adduct (R derived from AAPH): A. G. Krainev, T. D. Williams and D. J. Bigelow, *J. Magn. Res.*, *Ser. B*, 1996, **111**, 272.

29 H. Fujie, K. Shiraki, T. Miyagawa, N. Minamii, B. Yamada and T. Otsu, *Pure Appl. Chem.*, 1992, **A29**, 741. The decomposition was followed by UV at 50 °C. No hydrolysis problem was reported, however. This can be explained by the fact that the authors followed the decomposition only for the first 50 min.

30 A. I. Meyers, J. P. Lawson, D. G. Walker and R. J. Linderman, *J. Org. Chem.*, 1986, **51**, 5111.

31 The existence of two diastereomers is also proposed for the DEPMPO-OOH adduct. In the case of DMPO–OOH, Buettner was the first to propose similar effects in phosphate buffered solutions. See: G. R. Buettner, *Free Radical Res. Commun.*, 1990, **10**, 11.

32 Only very minor modifications such as shorter reaction times (2 days for synthesis of acetoxymercuridurene) were made. (*a*) For the mercuriation of durene see: L. I. Smith and F. L. Taylor, *J. Am. Chem. Soc.*, 1935, **57**, 2370; (*b*) For the subsequent nitrosation see: L. I. Smith and F. L. Taylor, *J. Am. Chem. Soc.*, 1935, **57**, 2460 and reference 8 therein.

33 The only available procedure does not describe the synthesis of MDN itself, but it reports the synthesis of derivatives of the MDN spin trap such as *N*-mesitylenemesitylamine *N*-oxide. See J. E. Baldwin, A. K. Qureshi and B. Sklarz, *J. Chem. Soc.*, 1969, 1073.

34 E. G. Janzen and B. J. Blackburn, *J. Am. Chem. Soc.*, 1969, **91**, 4481.

35 R. B. Cole, ed., *Electrospray Ionization Mass Spectrometry*, John Wiley and Sons, New York, 1997.

36 H. Iwahashi, *J. Chromatogr. A*, 1996, **753**, 235.

37 J. A. Weil, J. R. Bolton and J. E. Wertz, *Electron Paramagnetic Resonance, Elementary Theory and Practical Applications*, John Wiley and Sons, New York, Singapore, 1994.

38 B. Eistert, H. Fink, J. Riedinger, H. G. Hahn and H. Dürr, *Chem. Ber.*, 1969, **102**, 3111.

39 For synthesis of methyl acetimidate hydrochloride, see A. I. Myers, J. P. Lawson, D. G. Walker and R. J. Linderman, *J. Org. Chem.*, 1986, **51**, 5111.

40 E. G. Janzen, G. A. Coulter, U. M. Oehler and J. P. Bergsma, *Can. J. Chem.*, 1982, **60**, 2725.

Paper 8/01624K
Received 20*th February* 1998
Accepted 7*th June* 1998